

# EFM phase investigation of the metal–organic film interface

A. Das<sup>a,\*</sup>, C.H. Lei<sup>a</sup>, H.E. Thomas<sup>a</sup>, M. Elliott<sup>a</sup>, J.E. Macdonald<sup>a</sup>,  
P. Glarvey<sup>b</sup>, M.L. Turner<sup>b</sup>

<sup>a</sup> School of Physics and Astronomy, Cardiff University, 5 The Parade, Cardiff CF24 3YB, UK

<sup>b</sup> Organic Materials Innovation Centre, Department of Chemistry, University of Manchester, Manchester M13 9PL, UK

Available online 30 January 2006

## Abstract

Phase sensitive electrostatic force microscopy (EFM phase) investigations of semiconducting polymers, poly(3-hexylthiophene) (P3HT) and poly(9,9-dioctylfluorene) (F8), are described, aimed at understanding the metal/polymer interfaces. The electrostatic behaviour and potential distributions of the Au/polymer/Au structure under various biases with emphasis on top and bottom Au contacts are presented. We observe, by analysing EFM phase data, that the top and bottom contacts of Au can have drastic effects on the device performance. Moreover, differences in conductivity of conjugated polymers (P3HT > F8) are also reflected in EFM phase measurements, which correlate well with *I*–*V* measurements. Detailed analysis indicates that the influence of metal/film interfaces depends strongly on both the ability of charge transport properties of the organic films and the type of surface modification.

© 2005 Elsevier B.V. All rights reserved.

PACS: 36.20.–r; 73.40.Cg; 73.40.Sx

Keywords: Conjugated polymers; P3HT; F8; Electrostatic force microscopy; Metal contacts

## 1. Introduction

Use of conjugated polymers as the semiconducting layer in field effect transistors (FETs), solar cells and light emitting diodes (LED) offers the benefits of easy processability, low cost and flexibility. Soluble and processable P3HT and polyfluorenes have been found to be promising for organic based electronics [1,2]. P3HT is a conjugated polymer with the highest hole mobility found so far [3], and has been frequently employed as the semiconducting component in organic field effect transistors [4]. It has been reported that structural order and morphology of P3HT films can vary depending on the film processing conditions [5] and the mobility is affected by the structural ordering in the films. Polyfluorenes including poly(9,9-dioctylfluorene) are reported to show efficient blue electroluminescence (EL) [6,7], and are now attracting much interest due to their low turn-on voltage, high brightness, and high efficiency.

A critical issue for organic based devices is producing suitable metal contacts. The interface formed between a metal and an organic film can significantly influence the electrical properties of the system. Moreover, the magnitude of ordering and hence mobility of a film largely depends on the growth process regulated by the substrate surface. Therefore, understanding and control of the molecular alignment and morphology and their effect on the electronic transport properties of conducting polymers is crucial for further development of devices.

As the dimensions of electronic devices become ever smaller, the ability to characterise electrical properties at microscopic scales gains greater significance. Atomic force microscopy (AFM), together with electrostatic force microscopy (EFM), offers an important role in the electrical characterisation of integrated circuits and nanometre-scale devices. We have demonstrated that the EFM phase mode can deliver higher resolution down to the nanometer scale than conventional scanning Kelvin probe potential measurements (SKPM) [8]. The EFM phase mode can be applied to low conductivity semiconducting polymers where STM might not work. Measurement of the force gradient rather than the force itself [9] produces a higher resolution measurement of the surface potential. The phase shift is related to the surface

\* Corresponding author. Tel.: +44 2920874056; fax: +44 2920870166.

E-mail address: [spxad@cf.ac.uk](mailto:spxad@cf.ac.uk) (A. Das).

potential indirectly, so calibration of the EFM phase measurement is needed to provide quantifiable potential measurements.

Here we show the potential application of EFM phase investigations of semiconducting polymers (F8 and P3HT) and metal/polymer interfaces. Specifically, we compare two configurations: polymers spin coated on pre-defined Au electrodes on SiO<sub>2</sub>/Si substrates (bottom contact) and Au electrodes deposited on top of the spin cast polymer film (top contact). We probe the electrical potential profile across the interface showing the significant differences in the contact behaviour. Detailed analysis indicates that the influence of the metal/film interface depends strongly on both charge transport properties of the organic films and the type of surface modification.

## 2. Experimental

### 2.1. EFM phase measurement

In EFM phase measurements, a scanning force microscopy (AFM) tip performs a main scan and an interleave scan on each scan line. The main scan records the surface topographical data in tapping-mode and in the following interleave scan, which traces the topography at a fixed height above the surface, acquires the electrostatic data. A potential difference  $\Delta U$  between the tip and the surface gives, for small force gradients, a resonant phase shift of

$$\Delta\phi = -\arcsin\left(\frac{Q}{2k} \frac{d^2C}{dz^2} (\Delta U)^2\right) \quad (1)$$

where  $k$  is the spring constant and  $Q$  is the quality factor of the cantilever [8].  $C$  is the capacitance between the probe and the sample. The EFM feedback system records the phase shift which is a function of the potential difference  $\Delta U$  between the tip and the small area beneath the tip, because the tip apex gives the biggest contribution to the  $d^2C/dz^2$  value. This second derivative accentuates the effect of the tip apex rather than the cantilever and bulk of the tip, thus providing higher spatial resolution  $\sim 20$  nm [8]. In practical applications, calibration of the EFM phase system involves relating the phase shift directly to the local surface potential. This is performed on a flat surface, on which a series of potentials is applied and corresponding phase shifts are recorded, at a fixed scan height  $z$ . The data is fitted to the Eq. (2).

$$\Phi = -\arcsin[A(V - V_0)^2] + B \quad (2)$$

where  $A$  represents the constant parameter  $(Q/2k)(d^2C/dz^2)$  in Eq. (1),  $B$  represents the offset phase value when  $V = V_0$ , and  $V_0$  represents a bias offset, which arises mainly from the work function difference between the Si-probe and the Au film [9]. Once the phase–potential relationship has been obtained it is used to convert phase values to electrical potential across the sample. The EFM phase measurements were performed in ambient conditions with an SPM (NanoScope IIIa Multimode, Digital Instruments). An  $n^+$ -Si cantilever with a free-resonant

frequency and free tapping amplitude about 302 kHz and  $\sim 13$  nm, respectively was used and was connected to the electrical ground. The interleave scan lift height was 20 nm.

### 2.2. Sample preparation

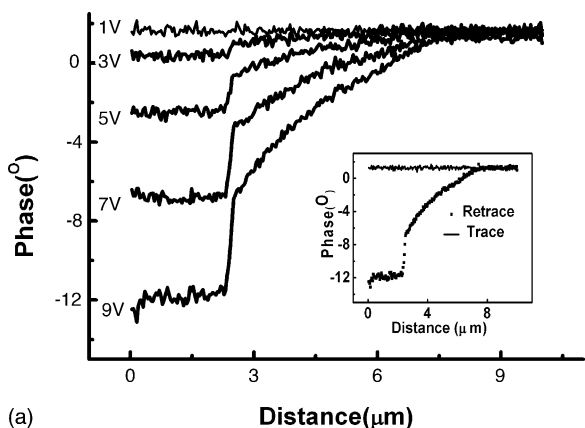
The polymer films were prepared by spin coating from toluene solvent for F8 (2 mg/ml). This procedure produced a uniform, continuous film with a thickness of  $\sim 6$  nm for F8. CHCl<sub>3</sub> solvent is used for P3HT (1 mg/ml) with a thickness of  $\sim 4$  nm. For the bottom-contact configuration, the polymer film was spun onto the Au/SiO<sub>2</sub>/Si substrate with pre-prepared Au electrodes. For the top-contact samples, Au electrodes were deposited on the spin coated polymer film by thermal evaporation. The evaporation rate of Au was  $\sim 0.2$  nm/s in a vacuum of  $\sim 4 \times 10^{-6}$  mbar. The Au electrodes in both samples were  $\sim 15$  nm thick,  $\sim 3$  mm wide and were separated by  $\sim 5$   $\mu$ m as described in [10]. The substrate is SiO<sub>2</sub>/Si with a typical oxide thickness 30 nm. For cleaning and producing a hydrophilic substrate, the surface is treated for 5 min in UV-ozone chamber (Bioforce, Nanoscience Inc.).

## 3. Results and discussion

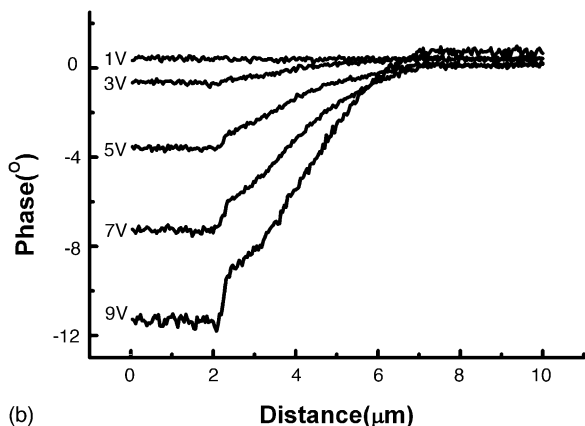
### 3.1. EFM phase measurement results

Following calibration, the phase measurements were used to quantify the potential distribution across the Au/polymer/Au structure. The EFM phase measurements were carried out on a fixed line 10  $\mu$ m long across the electrode gap region of the samples. A series of biases is applied to the left Au electrode with the right one grounded. The results are displayed in Fig. 1a and b for the top contact and the bottom contact F8 samples, respectively. Fig. 2 shows corresponding potential values obtained from the calibration process described above. In Fig. 3, EFM phase measurements for Au top and bottom contacts to P3HT film are displayed with 9 V applied to the left electrode. Ohmic behaviour is evident for the bottom contact while the top contact data indicate a rapid potential drop close to the electrode as shown by the two vertical lines in Fig. 3. This suggests that the electrical properties of P3HT film have been changed by thermal deposition of Au atoms. A more detailed discussion can be found elsewhere [10].  $I$ – $V$  measurements for both configurations are consistent with this behaviour. The recorded conductivity for the top contact is an order of magnitude lower than the bottom contact configuration [10].

Figs. 1 and 2 depict phase and voltage data of bottom and top contacts, respectively for F8 polymer. For F8, both top and bottom configurations display a potential drop at the interface region. There are distinct differences for F8 compared with P3HT. Firstly, the bottom contact of F8 shows a sudden change at the contact region in contrast to a gradual drop in potential following an ohmic contact for P3HT. In general, high resistance at the left electrode edges is prominent for both top and bottom contacts of F8. Secondly, F8 does not show as marked changes at the electrode edge as observed for P3HT



(a)

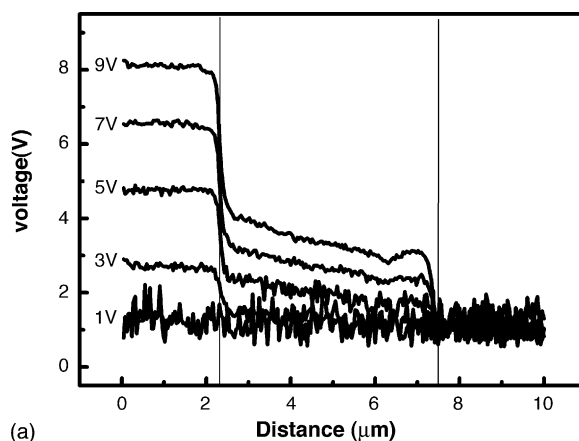


(b)

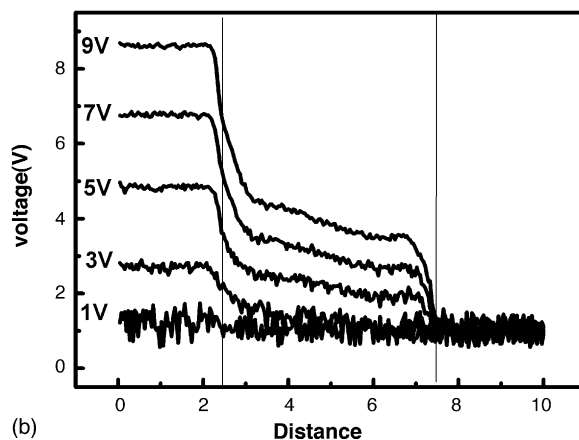
Fig. 1. EFM phase data of F8 (UV-ozone treated SiO<sub>2</sub>/Si substrate) across the gap region with a series of biases with two configurations: (a) top and (b) bottom contacts.

samples after Au atom deposition. However, F8 clearly shows a sharper potential drop at the electrode edge for the top contact than for the bottom contact. Moreover, the bottom contact of F8 shows a steep drop in potential for nearly 1 μm length at the contact in the gap region followed by a more gradual monotonic fall in potential due to the resistance of polymer film extended to the right electrode. The sharp drop at the electrode edge might have resulted from a combination of many influencing factors e.g. the sudden work function change from Au electrode to polymer, a large resistance metal/polymer contact, possible interface dipole formation or band bending and a possible cross talk due to the height change between the Au electrode and the gap region. Topographic cross talk can be ruled out since it is not observed for similar topography for P3HT/Au contacts.

I–V measurements carried out on these F8 samples, however, did not show any significant detectable current (less than ~pA) under a bias up to 20 V, indicating the very low conductivity arising from low charge mobility and/or its concentration. Ohmic P3HT/Au contact can be achieved (Fig. 3), because of a compatible work function with Au (~4.8 eV) [9]. P3HT has an ionization potential (IP) of 4.3 eV [11]. In contrast, F8 has IP at ~5.8 eV [6] and a band gap of 3.1 eV [12] giving lower conductivity and creating a barrier to carrier injection from Au.



(a)



(b)

Fig. 2. The potential distribution of F8 (UV-ozone treated SiO<sub>2</sub>/Si substrate) across the gap region with a series of biases, obtained by EFM/phase method with two configurations: (a) top and (b) bottom contacts.

### 3.1.1. Influence of substrate

It is known that polymer morphology is largely dependent on the substrate conditions which can considerably influence the mobility of the charge carrier [13]. Fig. 4 shows the EFM phase measurements of F8 on SiO<sub>2</sub>/Si substrate without any UV-ozone treatment for the top contact configuration. The inset in Fig. 4 displays the trace and the retrace scans for a 9 V bias. No

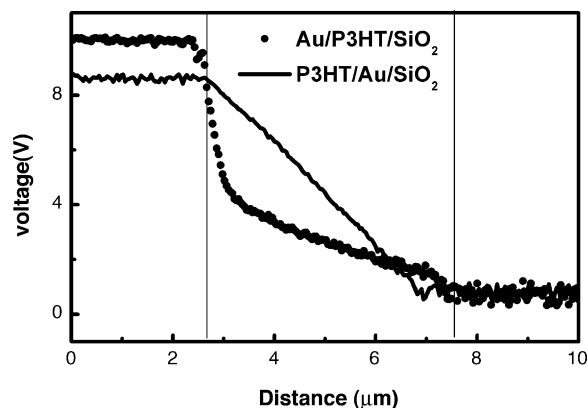
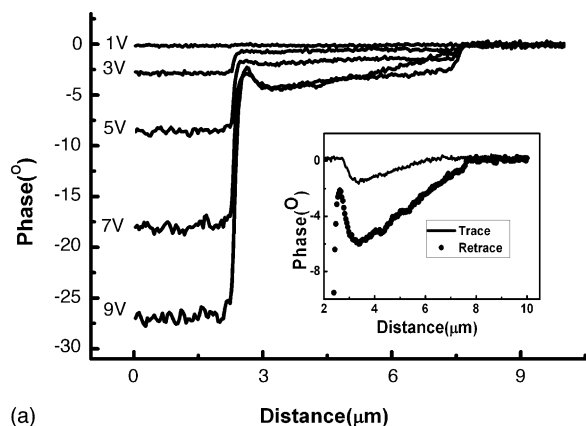
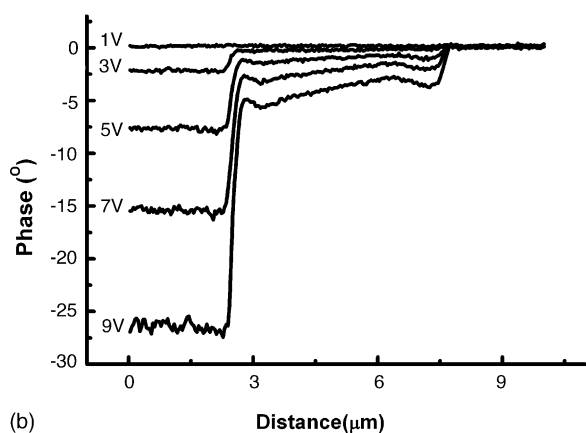


Fig. 3. The potential distribution of P3HT on SiO<sub>2</sub>/Si substrate, across the gap region with a 9 V bias, obtained by EFM/phase method, with two configurations, top (circles) and bottom (line) [10].



(a)



(b)

Fig. 4. EFM phase data of F8 ( $\text{SiO}_2/\text{Si}$  substrate) across the gap region with a series of biases with two configurations: (a) top and (b) bottom contacts.

bias was applied during the trace scan, but a significant phase shift was still observed during the trace scan. This is possible if the charges injected during the retrace scan remained in the polymer film contributing towards the phase shift during the following trace scan. This is clear evidence of local charge trapping observed at 9 V for the top contact on  $\text{SiO}_2/\text{Si}$  substrate. Such an effect could not be directly identified for low voltages for UV-ozone treated substrates (onset in Fig. 1). This indicates high concentration of charge trapping and low charge mobility of F8 on  $\text{SiO}_2$  substrate in contrast to F8 films on UV-ozone treated substrates. This might be result of higher degree of amorphous or randomly oriented polymer chains which can trap charges on  $\text{SiO}_2$  substrates. Further evidence of charge trapping in the bottom contact configuration of F8 was obtained by applying a gate voltage to the UV-ozone treated substrates. However, the issues of gate voltages and charge trapping in polymer films will be discussed in future communications.

For F8 samples, a prominent hump structure at the electrode edges (Figs. 2 and 4) could be seen at higher bias voltages, 7 V or above. This indicates local negative impedance behaviour. Low conductivity and charge mobility have been already evident from  $I$ – $V$  measurements and EFM phase investigations for F8 samples. These humps in the F8 sample could be the result of accumulated charge on the electrode edges because of very low mobility of charges created during the EFM phase measurements with the biased Au electrode. The high conductivity of P3HT films did not

build up charges and consequently, no such humps at the electrode edges could be seen.

#### 4. Conclusions

High resolution surface potential measurement by EFM phase has been used to characterise electronic properties of conjugated polymers, with a simple polymer–Au contact structure. Comparison was made between the polymers F8 and P3HT, top and bottom contacts.  $I$ – $V$  measurements indicate high conductivity of P3HT films compared to F8 polymer. EFM phase measurement of the bottom contact of P3HT shows Ohmic behaviour and the top contact has a high resistance close to the Au–P3HT contact due to the defects. In contrast to P3HT films, both top and bottom contacts of F8 polymer films produce a high resistance region close to the Au–F8 contact as revealed by EFM phase measurements. Moreover, this high resolution technique can distinguish a sharper potential drop at the electrode edge for the top contact of F8, possibly originating from similar reasons as observed for the P3HT films than for the bottom contact of F8 film. Additionally, the ability of the EFM phase approach to measure and characterise the influence of substrate surfaces like the trapped charges in the F8 film on the untreated  $\text{SiO}_2/\text{Si}$  substrates in contrast to the UV-plasma treated  $\text{SiO}_2/\text{Si}$  substrates is clearly advantageous for investigating the charge transport properties of semiconductor polymers related to their structures, and the use of these materials as the electronically-active layer in devices.

#### Acknowledgments

The authors would like to thank the technical and computing support staff of this department for help in sample preparation and technical support. This research has been partially supported by the EPSRC, grant GR/S02280.

#### References

- [1] Z. Bao, A. Dodabalapur, A.J. Lovinger, *Appl. Phys. Lett.* 69 (1996) 4108.
- [2] Q. Pei, Y. Yang, *J. Am. Chem. Soc.* 118 (1996) 7416.
- [3] H. Sirringhaus, N. Tessler, R.H. Friend, *Science* 280 (1998) 1741.
- [4] L. Burgi, H. Sirringhaus, R.H. Friend, *Appl. Phys. Lett.* 80 (2002) 2913.
- [5] H. Sirringhaus, P.J. Brown, R.H. Friend, M.M. Nielsen, K. Bechgaard, B.M.W. Langeveld-Voss, A.J.H. Spiering, R.A.J. Janssen, E.W. Meijer, P. Herwig, D.M. de Leeuw, *Nature* 401 (1999) 685.
- [6] S. Janietz, D.D.C. Bradley, M. Grell, C. Giebeler, M. Inbasekaran, E.P. Woo, *Appl. Phys. Lett.* 73 (1998) 2453.
- [7] M.J. Banch, R.H. Friend, H. Sirringhaus, *Macromolecules* 36 (2003) 2838.
- [8] C.H. Lei, A. Das, M. Elliott, J.E. Macdonald, *Appl. Phys. Lett.* 83 (2003) 482.
- [9] C.H. Lei, A. Das, M. Elliott, J.E. Macdonald, *Nanotechnology* 15 (2004) 627.
- [10] C.H. Lei, A. Das, M. Elliott, J.E. Macdonald, M.L. Turner, *Synth. Met.* 145 (2004) 217.
- [11] R.P. Mikalo, D. Schmeißer, *Synth. Met.* 127 (2002) 273.
- [12] L.S. Liao, M.K. Fung, C.S. Lee, S.T. Lee, M. Inbasekaran, E.P. Woo, W.W. Wu, *Appl. Phys. Lett.* 76 (2000) 3582.
- [13] N. Zhao, G.A. Botton, S. Zhu, A. Duft, B.S. Ong, Y. Wu, P. Liu, *Macromolecules* 37 (2004) 8307–8312.